


ARTICLE

Forcespun polyvinylpyrrolidone/copper and polyethylene oxide/copper composite fibers and their use as antibacterial agents

Md Toukir Hasan¹ | Ramiro Gonzalez¹ | Ari Alexis Munoz² | Luis Materon² | Jason G. Parsons³ | Mataz Alcoutlabi¹ 

¹Mechanical Engineering Department, University of Texas Rio Grande Valley, Edinburg, Texas, USA

²Department of Biology, University of Texas Rio Grande Valley, Edinburg, Texas, USA

³Department of Chemistry, University of Texas Rio Grande Valley, Brownsville, Texas, USA

Correspondence

Mataz Alcoutlabi, Mechanical Engineering Department, University of Texas Rio Grande Valley, Edinburg, TX, USA.

Email: mataz.alcoutlabi@utrgv.edu

Funding information

UTRGV; National Science Foundation (NSF) PREM award, Grant/Award Number: DMR-2122178

Abstract

Copper nanoparticles (CuNPs) embedded in polyvinylpyrrolidone (PVP) and polyethylene oxide (PEO) fiber-matrices were prepared through centrifugal spinning of PVP/ethanol and PEO/aqueous solutions, respectively. The prime focus of the current study is to investigate the antibacterial activity of composite fibers against *Escherichia coli* (*E. coli*) and *Bacillus cereus* (*B. cereus*) bacteria. During the fiber formation, the centrifugal spinning parameters such as spinneret rotational speed, spinneret to collector distance, and relative humidity were carefully chosen to obtain long and continuous fibers. The structural and morphological analyses of both composite fibers were investigated using scanning electron microscopy, X-ray diffraction, energy-dispersive X-ray spectroscopy, and thermogravimetric analysis. In the antibacterial test, PVP/Cu and PEO/Cu composite fibrous membranes exhibited inhibition efficiency of 99.98% and 99.99% against *E. coli* and *B. cereus* bacteria, respectively. Basically, CuNPs were well embedded in the fibrous membrane at the nanoscale level, which facilitated the inhibition of bacterial functions through the inactivation of the chemical structure of the cells. Such an effective antibacterial agent obtained from forcespun composite fibers could be promising candidates for biomedical applications.

KEYWORDS

biomedical applications, centrifugal spinning, fibers, nanocrystals, nanoparticles, nanowires, thermogravimetric analysis

1 | INTRODUCTION

Nowadays, microorganism (e.g., gram-positive and gram-negative bacteria) originated from spoilage or contaminated products is rampantly affecting the compositional change of human intestine negatively^{1,2} by which the tissue interlink system can collapse.³ Correspondingly, for the protection from microorganisms, efficacious antibacterial agents, developed from suitable metal/polymer nano-

composites, have been widely used to impede bacterial cell proliferation due to having higher efficiency, stability, biocompatibility, biodegradability, and availability to process.⁴⁻⁶ Fortunately, human skin is coherently compatible with the morphological characteristics of nanofibrous membrane,^{7,8} facilitating the inhibition of bacteria through absorbing exudates.⁹⁻¹¹

Nanotechnology promotes to develop nanofibers conveying high-specific surface area to volume ratio, surface

composition¹² and higher porosity with functional additives where the interfacial strength of layers is congruent to the size, shape, and composition of the nanofibers. In general, the antibacterial ability of a fibrous membrane is a variable function of the surface area in contact with the bacterial layers.¹³ Conceptually, nanofibers react significantly with the bacterial surface because of their high-surface area and porosity. Zupančič et al.¹⁴ reported that thicker nanofibers can reduce the bacterial cell mobility more profusely and quickly than thinner fibers as the response was cell-line specific.^{15,16} Therefore, nanofibers can exhibit strong inhibition performance and be used as antibacterial agents^{17,18} in drug delivery,^{19,20} tissue engineering,^{21–23} bio-adhesive,²⁰ and filtration.

Nano/micro fibers can be prepared by various processing methods such as melt blowing, electrospinning,^{24–26} centrifugal spinning,^{27–34} dry spinning,³⁵ phase separation,³⁶ and self-assembly.³⁷ Centrifugal spinning or forspinning (FC) has been recently used to produce fibers at a high-production rate (1 g/min) and low cost^{32,33,38} where both conducting and nonconducting solutions/melts can be centrifugally spun into fibers.^{29,39} Beyond these features, for an identical solution at ambient conditions, centrifugally spun fibers yield more porous-based shape than electrospun fibers.^{14,40}

Several polymer systems have been recently centrifugally spun into fibers.^{41,42} Likewise, polyethylene oxide (PEO) and polyvinylpyrrolidone (PVP) polymers have been forspun to generate fibers for various applications. Both polymers are soluble in water and/or other solvents,⁴³ biodegradable, biocompatible,⁶ physiologically acceptable polymers and nontoxic for living organisms.⁴⁴ For PVP/ethanol solution, oxygen adjoins with hydrogen of ethanol⁴⁵ while for aqueous PEO solutions, PEO reacts with water to lead to a weak hydrogen bond.⁴⁶ Consequently, this bond increases solubility with the flexible polymer long chains. Because of the hydrophilic nature of such long structural chains, both polymers prevent protein adsorption⁴⁷ of bacterial responses.⁴⁸ As a whole, both PVP and PEO fibrous membranes are good capping agents, assisting charge transfer to inhibit bacteria efficiently.⁴⁹

It has been experimentally observed that PEO composite fibers with chitosan and embedded Ag nanoparticles (AgNPs) exhibited good inhibition zone against *Staphylococcus aureus* (*S. aureus*) and *Klebsiella pneumoniae* bacteria.^{50,51} On the other hand, well functionalized PVP/ZnO nanocomposites were fabricated via electrospinning for use as an antimicrobial agent.⁵² Apart from PEO and PVP fibers, Yalcinkaya et al. reported that the inhibition efficiency of polyvinyl butyral (PVB)/CuO was over 90% (much higher) since cupric (Cu^{2+}) ions can be distributed more homogeneously in the fibrous membrane.⁵³ According to the comparison of antibacterial performance between

Chitosan and PVP/ZnO composite fibers, Karpuraranjith et al., showed that PVP/ZnO inactivated gram positive and negative bacteria 17% and 6% more than that for chitosan, respectively. Additionally, compared to Chitosan, Chitosan/PVP/ZnO nanocomposites increased the inhibition zone by 42% more against *Escherichia coli* (*E. coli*). The reason behind this is that higher inhibition was possible because the effective capping agent, PVP fibers provided higher surface area where Zn NPs were evenly distributed to spoil biocidal activity.⁵⁴ Moreover, thermally, and chemically reduced Ag NPs embedded in PVP fiber-matrix promoted the uniform agglomeration of Ag NPs, assisting to interlink to a coordination bond with PVP ($-\text{N}$ or $-\text{O}$).⁵⁵ Higher molecular weight PVP tends to pattern uniform fibers with a smaller diameter distribution, eventually results in good interaction with NPs and exhibiting improved antimicrobial properties.³

The microbial cell of bacterial strains attributes to very less longevity to ZnO, Ag, and copper nanoparticles (Cu NPs).¹ Throughout experiments, the inhibition efficiency of different heavy metal NPs has been investigated where the order of antibacterial activity against *E. coli* was demonstrated as following: $\text{CuO} > \text{ZnO} = \text{ZnO}/\text{TiO}_2 > \text{AgNO}_3 > \text{ZrO}_2 > \text{TiO}_2 > \text{SrO}_2$.⁵⁶ It is noticeable that PVB/CuO composites showed good results since the smallest diameter (244 nm) and high-surface porosity (60.6%) of CuO⁵⁶ could accelerate well emendation in the fiber's membrane. Being inspired from these results, Ren et al. reported results on the antibacterial activities of CuNPs in that the CuNPs at higher concentrations could kill a wide range of bacterial pathogens.^{57,58} In fact, CuNPs have higher surface area, catalytic properties, good biocompatibility, stability, and reactivity than AgNPs⁵⁹ which prompts to form Cu^{2+} to dysfunction bacterial enzyme.^{3,60} More importantly, Cu is an engrossing antimicrobial agent because it is relatively cheap, easily mixed with polarized liquid and polymers.⁶¹

The focus of the present work is to investigate the antibacterial functionalities of centrifugally spun PEO/Cu and PVP/Cu composite fibers against *E. coli* and *B. cereus* bacteria. CuNPs are very reactive and perilous to human body because of which nanofibrous membrane intermingled with CuNPs may potentially be favorable for drug delivery and healing agent for human body. Typically, AgNPs are good antibacterial agent, however in this study, CuNPs were harnessed as an another alternative antibacterial agent, which are less expensive, highly active and more stable than AgNPs.⁵⁹ The present work focused on the capability, functionality, dissolution, and feasibility of centrifugally spun PEO/Cu and PVP/Cu composite fibers as a novel case to visualize the antibacterial activity. More importantly, the premise behind the study was to determine the optimum Cu

concentration in fibers for the dysfunctionality of microbial attack. For this reason, two different polymers, PEO and PVP were selected since both are biocompatible, biodegradable and easily dissolved into very cost-effective solvents (water, ethanol). Additionally, the analysis based on the various experiments verified whether PEO or PVP fibers encapsulation of Cu NPs was feasible and if these fibers exhibit antibacterial inhibition at a various concentration of Cu.

2 | EXPERIMENTAL

2.1 | Materials

PEO and PVP with average Mw of 600,000 and 1,300,000 were purchased from Sigma-Aldrich (St. Louis, MO, USA) and the solvent comprised of 100% pure deionized water (distilled water) and ethanol. CuNPs with sizes of 40–50 nm were obtained from US Research Nanomaterials, Inc (Huston, TX, USA). All chemicals were used as received without further purification.

2.2 | Preparation of polymer/nanoparticles composite fibers

PEO 8% (wt/wt) and PVP 18% (wt/wt) were dissolved in water and in ethanol, respectively. The solution was agitated by a Fisherband™ Analog Vortex mixer at 3200 rpm and then CuNPs of 15, 25, and 35 wt% concentration, with respect to the polymer, were added to the solution. After the mixture was sonicated by Cole-Parmer 08895–12 Ultrasonic cleaner at 40°C for 1 h, the solution was then magnetically stirred by Thermo Scientific Cimarec+4x4 HP120, Cimarec Stirring Hotplates at 25°C for 96 h. The rotational speed of the stirring plate was 400 rpm. The proper homogeneous PEO/Cu and PVP/Cu solutions were then centrifugally spun using Cyclone L-1000 M (Fiberio Technology Corporation) to produce the composite fibers. The as-prepared polymer solutions were injected into a spinneret equipped with 30-gauge half-inch regular bevel needles. Adequate centrifugal forces were applied to the precursor solution to exceed the surface tension of the polymer jets and stretch out the fibers.^{30,31,41,62,63} Centrifugal spinning was performed based at rotational speeds of 5000 rpm for PEO aqueous solution and 7500 rpm for PVP solution and at a relative humidity of 46%. The fibers were then collected in a well-arranged eight uniform spacious vertical collectors while the collector was set at 12 cm from the spinneret. The PVP/Cu and PEO/Cu composite fibers were then kept in an Al foil and dried at 60°C for 24 h in a vacuum oven.

2.3 | Characterization

The morphology of PVP/Cu and PEO/Cu composite fibers was studied by scanning electron microscopy (FE-SEM; Sigma VP Carl Zeiss, Germany). Before conducting the SEM analysis, the samples were sputtered with a thin layer of gold coating using a Denton's Desk V deposition system to obtain high-quality images. Then the average diameter of the samples was calculated from SEM images with 5 KX resolution by measuring 150 counts of various images using the image analysis software JMicroVision V.1.2.7 (University of Geneva, Geneva, Switzerland) and Origin Pro® 2020 software.

Energy-dispersive X-ray spectroscopy (EDS) analysis (EDAX, Mahwah, NJ, USA) was performed to evaluate the elemental composition of C, O, N, and Cu NPs in the fibers. The elemental composition of other different elements was scrutinized thoroughly for six of the samples where different areas were identified and peaks were obtained accordingly to those areas.

Thermogravimetric analysis (TGA) analysis of PVP/Cu and PEO/Cu composite fibers was investigated by TA-Q series equipment, TGAQ500 (TA Instruments Inc.) under air environment. Samples of about 10 mg were kept in the instrument and heated from 25 to 700°C under air flow at a heating rate of 5°C/min.

X-ray diffraction (XRD) analysis was performed on the composite fibers to determine the crystal structure. A Bruker D2 powder (Bruker Germany) X-ray diffractometer was used with a Co source ($K\alpha$ 1.789 Å), which was filtered using iron. The data were collected in 2θ from 10 to 80° with a count time of 5 s and a step of 0.05° in 2θ .

Antibacterial activities against the gram-positive bacteria *B. cereus* and gram-negative bacteria *E. coli* were evaluated for both PVP/Cu and PEO/Cu composite fibers. The most standard antibacterial performance measurement method, Kirby Bauer disk diffusion method, was used where Agar plate was kept, and then the bacterial suspension was uniformly outspread onto the surface of agar plates by a sterile L-shape glass rod. The fibrous mats were then stored on the surface of agar plates to evaluate the inhibition zone of bacteria. During this test, the fibers were incubated at 37°C for 72 h.

In vitro release experiments were performed to determine the Cu release and sample stability. The Cu-NPs, PEO/Cu, and PVP/Cu composite-fiber samples were suspended in 10 ml of deionized water (resistance 18 MΩ). The samples were placed on nutating mixer and equilibrated for 24 h. Subsequent to equilibration, the samples were then removed and centrifuged at 3000 rpm for 5 min and a 0.5 ml aliquot was extracted in triplicate. The extracted samples were saved and stored at 4°C prior

to analysis. The remaining samples were resuspended and placed back on the rotating mixer and equilibrated for additional 24 h. This sampling and resuspending procedure was repeated every 48 h for 7 days. The Cu concentration (released from the sample) was measured using Perkin Elmer 8300 Optima ICP-OES. The operating conditions of the ICP-OES were as follows: wavelength of 324.7 nm, nebulizer flow of 0.65 L/min, plasma flow of 20 L/min, an auxiliary flow of 0.2 L/min, and RF power of 1500 W while an integration time of 20 s was used per replicate. The data analysis was performed in triplicate.

3 | RESULTS AND DISCUSSIONS

3.1 | Morphology and structure of fibers

The finest structure and morphology of the centrifugally spun Cu/PEO and Cu/PVP composite fibers were obtained from the selective spinneret rotational speed, polymer concentration, viscosity, relative humidity, and the spinneret-to-collector distance. The effective combination of these parameters results in bead-free and uniform nanofibrous matrix. During centrifugal spinning, PEO aqueous solution of 8 wt% concentration⁴² produces bead-free fibers. In the case of PEO solution, the viscosity at 8 wt% concentration⁴² was very low to produce good fibrous mats whereas a higher viscosity than this one yielded beaded and torn fibers.⁶⁴ Here the experiments were performed at 46%–48% the relative humidity since aqueous solution did not get evaporated beyond upper of this humidity. Mostly in that case, enough vapors could not suck out existent water from the solution. During centrifugal spinning of PEO/Cu composite fibers, the spinneret rotational speed was set between 5500 and 8000 rpm at a favorable humidity. However, the centrifugal spinning of PEO/Cu solutions at rotational speeds lower than 4500 rpm barely produced morphologically uniform fibers due to the high-surface tension of the polymer droplets.⁶⁵ Conversely, at rotational speeds above 9000 rpm, the centrifugal forces exceeded the solution's surface tension and resulted in fiber breakage.^{33,66} As a result, at shorter spinning time, more jets were ejected onto the collector swiftly and negatively affected the deposition of fibers on the collector. Finally, PEO/Cu solutions with 15, 25, and 35 wt% CuNPs were centrifugally spun to obtain uniform and layered fibers. Similarly, the PVP/ethanol solution was more favorable to be spun at 21 wt% concentration. Solutions having concentrations lower than 21 wt% were difficult to get fibers as the viscosity was lower while concentrations more than 28 wt% were cumbersome to spin. For the spinneret rotational speed, 7500 rpm was a good value to get fine fibers

at a favorable humidity. Experimentally, PVP/Cu solutions were centrifugally spun at 7500 rpm for three different Cu concentrations of 15, 25, and 35 wt%, which resulted in fibers with different morphologies. Figure 1 shows the SEM images of PEO/Cu composite fibers. The fibers (Figure 1a,c,e) were uniform, slender, and well-arranged. The histograms in Figure 1b,d,f clarify that the diameter of PEO/Cu composite fibers decreased with increasing the CuNPs loading in the PEO-fiber matrix, which was in agreement with previous experimental results.⁴² The SEM image in Figure 1c showed bundled PEO/Cu composite fibers. Several factors can lead to the formation of bundled fibers such as the distance between the collector and spinneret, solvent evaporation rate, vapor pressure of the solvent and van der Waals attraction between fibers.⁶⁷ A short distance between the spinneret and collector (12 cm in the present setup, which is the maximum distance) results in the formation of wet fibers that can easily bundle together on the collector. In fact, a slow evaporation rate of the solvent (e.g., water or DMF) will lead to the formation of wet fibers and once they are deposited on the collector, the fibers start to bundle. Using a solvent with high-vapor pressure such as ethanol, acetone and chloroform can increase the evaporation rate and hence reduce the adhesion between the fibers. Therefore, increasing the spinning time, collector-to-spinneret distance, temperature, and time of evaporation of the solvent can reduce the adhesion between fibers and ultimately prevent the formation of bundled fibers. Future work in our group will focus on the effect of solvent-type and binary solvent mixtures on the fiber formation and morphology of centrifugally spun composite fibers.

Furthermore, the SEM image in Figure 1 A showed that the fibers were lightly deformed from a cylindrical shape. The deformation may be due to the higher spinning speed with a shorter run time. In fact, polymer droplets might not have had enough time to be swelled and stretched properly at room temperature, which resulted in loss in the capability to softening into cylindrical shape properly.⁶⁸ Naturally nano/micro fibrous mats can be broken up due to lower vapor pressure of solvent where coalescing fibrous layers get lost due to easier relaxation of polymer chains into non-stretched conformation at slow drying process.⁶⁹ Additionally, the jet can break up due to viscous force, imbalance of centrifugal forces and surface tension. Furthermore, centrifugal and air drag forces can break up fibers from solutions with low viscosity where stretching was impeded and torn away.^{70,71} In addition, in centrifugally spinning the fibers are more loosely packed than in electrospinning because of the absence of the electric force field.⁷² Considering all reasoning for fiber deformation/breakage it may be clear

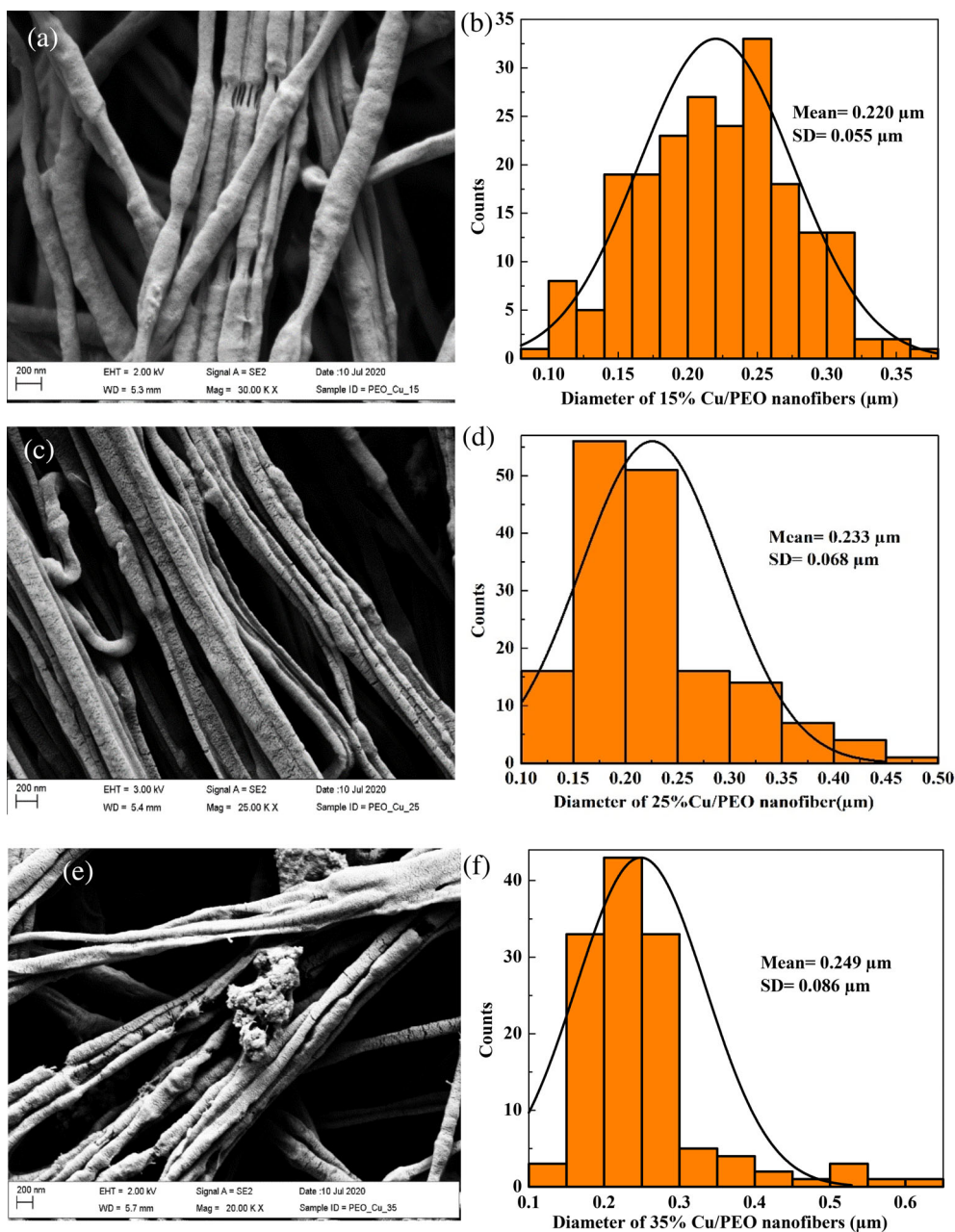


FIGURE 1 SEM images of the PEO/Cu and PVP/Cu composite nanofibers with 15, 25, and 35 wt% Cu NPs concentrations in the precursor solution ([a, c, e], [g, i, k]) respectively. The average fiber diameter distribution (histograms) ([b, d, f], [h, j, l]). Cu NPs, copper nanoparticles; PEO, polyethylene oxide; PVP, polyvinylpyrrolidone; SEM, scanning electron microscope [Color figure can be viewed at wileyonlinelibrary.com]

that at 15 wt% PEO/Cu precursor solution, the viscosity was lower, which led to the breaking of fibers in some parts, which was noticed.

Moreover, the SEM images shown in Figure 1a,c,e,g,i,k confirmed that the increase of Cu concentration in the PEO and PVP solutions resulted in bead-free PEO/Cu and PVP/Cu composite fibers. Basically, the metal nanoparticles (Cu NPs) assisted in reducing the crystallinity of the polymer as well as shortened the size of

crystallites of spherulites.⁷³ Eventually, the Cu NPs can disrupt the crystal portion and increase the amorphous region in the polymer matrix to enhance smoother morphology. PEO/Cu nanofiber's diameter ranged from 220 to 249 nm while the PVP/Cu nanofiber's diameter was within 4900–5500 nm (Figure 1a,c,e,g,i,k). Higher Cu concentrations in the polymer solution resulted in fibers with higher average fiber diameters as observed in the diametrical statistical analysis (histograms). The Cu

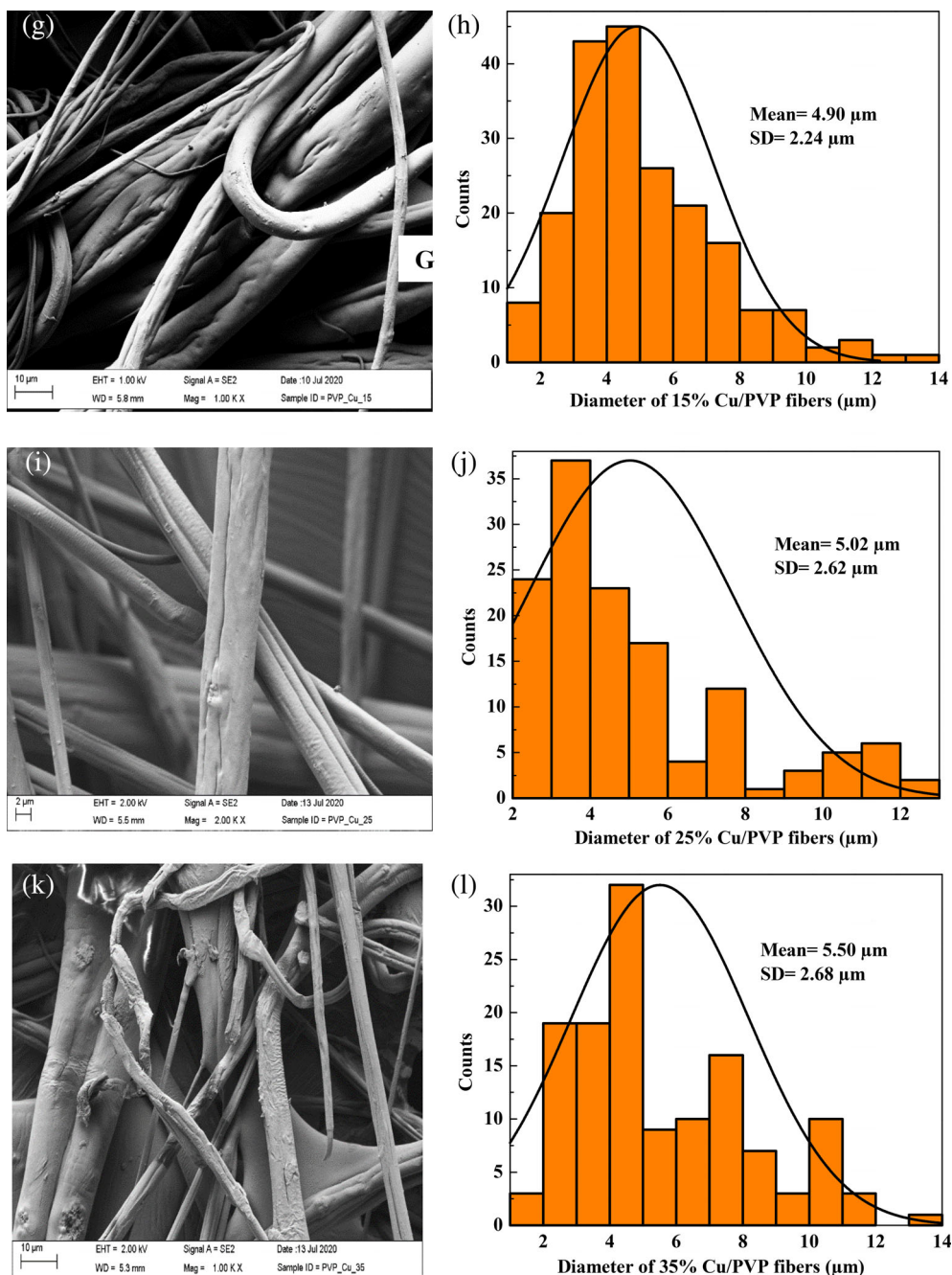


FIGURE 1 (Continued)

NPs were mainly embedded into the core/shell of fibers as well as attached to the outer surface of the nano fibrous membrane. If NPs were attached to the outer surface, then the NPs sometimes tended to agglomerate to form clusters on the fiber surface. From the morphological surface analysis, PEO/Cu fibers (Figure 1a,c,e) were flatter and thinner than PVP/Cu fibers (Figure 1g,i,k). As a semi-crystalline polymer, PEO with water as the solvent gets enough advantages to disperse more and keeps its crystallinity while the amorphous phase of PVP fibers

makes its nanofibrous membrane disordered and bended in various portion (Figure 1i,k).

3.2 | Elemental mapping analysis

EDS analysis was performed to investigate the elemental composition of the PEO/Cu and PVP/Cu composite fibers. Figure 2 shows the EDS mappings of 15 wt% Cu/PVP composite fibers. Based on a short sample area,

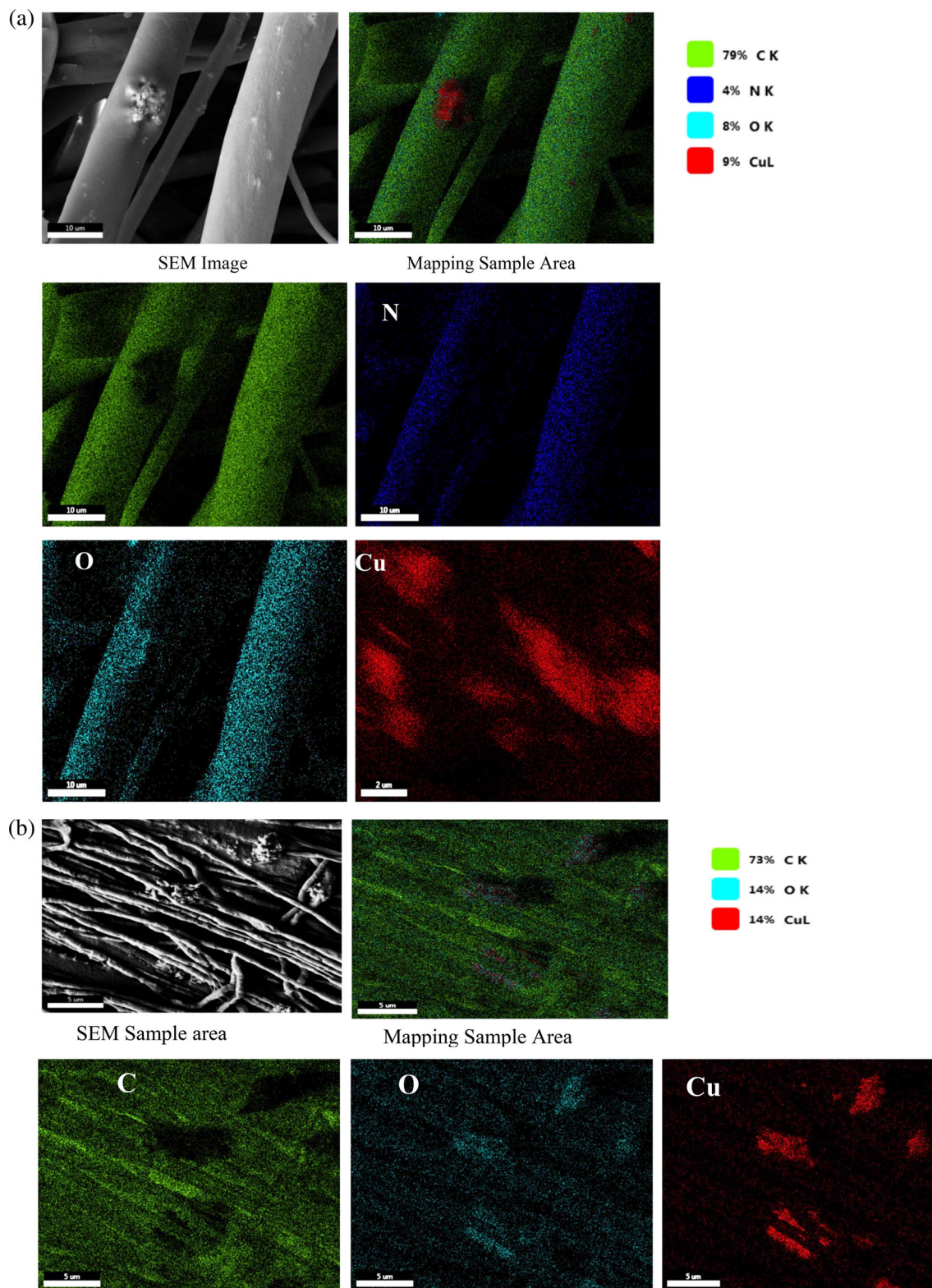


FIGURE 2 (a) Elemental composition of PVP/Cu nano-fibrous membrane. (b) Elemental composition of PEO/Cu nano-fibrous membrane. Cu, copper; PEO, polyethylene oxide; PVP, polyvinylpyrrolidone [Color figure can be viewed at wileyonlinelibrary.com]

the presence of C, N, O, Cu are detected as 79, 4, 8, and 9 wt% respectively, according to their composition percentages. Similarly, Figure 2b indicates the elemental

composition of 15 wt% of Cu/PEO composite fibers where C, O, and Cu are present in 73, 14, and 14 wt% respectively.

The EDS mappings in Figure 2a,b clearly show the presence of Cu, C, O, and N elements embedded in the PVP and PEO fibers.

3.3 | Thermogravimetric analysis

Thermal degradation of the PEO/Cu and PVP/Cu composite fibers was investigated by TGA under air environment. PEO/Cu and PVP/Cu composite fibers of 15, 25, and 35 wt% Cu concentrations (Figure 3) represent similar congruity in the TGA results with few changes caused by the addition of Cu NPs variously. At a temperature between 25 and 700°C; the weight loss of fibers was vividly apparent because of the thermal ignition. The pristine PEO fibers were almost volatilized completely at about 550°C, with a low amount of char being noticed (Figure 3a) while the pristine PVP fibers were vaporized finely at 600°C.

At a temperature range between 25 and 200°C, 3% weight loss of PEO fibers was caused by water evaporation to form anhydride while in the case of PVP fibers,

ethanol was quickly vaporized within this temperature range since PVP has more vapor pressure than water (Figure 3a). Basically, due to solvent disappearance, the polymer matrix suffers from volume shrinkage and its morphology gets vertical where nanofillers, CuNPs are not affected. Therefore, the peak at 80°C (Figure 3c) represents the removal of ethanol physically absorbed by the PVP-fiber surface.⁷⁴ In the second temperature region from 200 to 400°C, the weight loss of the PEO/Cu nanocomposite fibers is highly noticeable where the internal polymeric matrix loses weight during the thermal degradation. In this section, PEO loses its branching and cross-linking in order to initiate release chain scission.⁷⁵ Overall, the small cross-sectional area of fibers prepared from aqueous PEO solutions contributes to the semi-crystalline phase, which also turns to fully degraded as losing polymeric chains.⁷⁶ On the other hand, for PVP/Cu nanocomposite, the polymer fibers get more thermally decomposed from 250 to 450°C. In fact, PVP is an amorphous polymer whose disordered polymer chain is more thermally stable. As a result, PVP decomposes its chemical structure after a significant temperature change

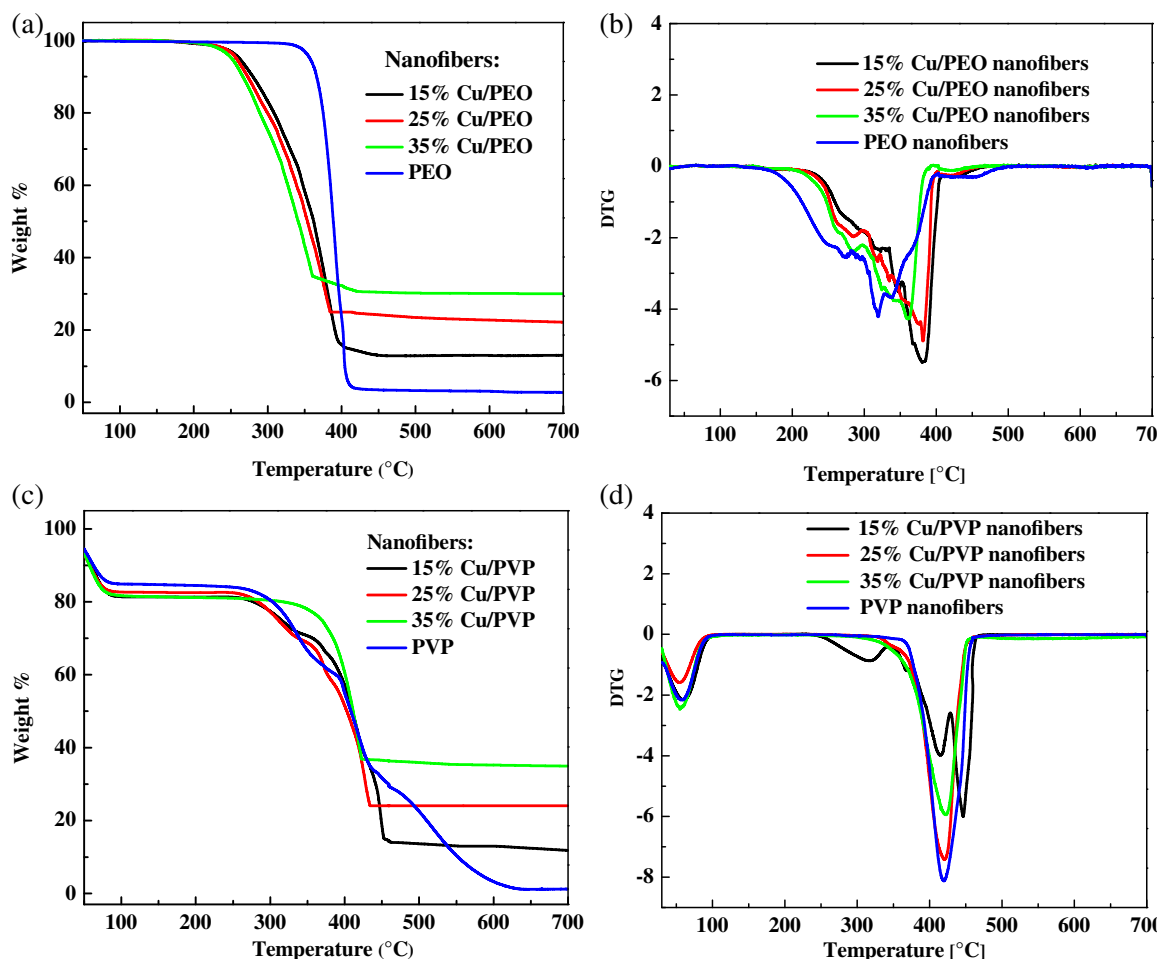


FIGURE 3 Thermal gravimetric analysis of (a) PEO/Cu and (c) PVP/Cu nanofiber. Gravimetric thermal derivative analysis of (b) PEO/Cu and (d) PVP/Cu. Cu, copper; PEO, polyethylene oxide; PVP, polyvinylpyrrolidone [Color figure can be viewed at wileyonlinelibrary.com]

as indicated in Figure 3c. Therefore, PVP fibers under oxidation at 300–400°C yields carbon dioxide and pyrrolidone which is apparent at the TGA peaks (350°C) terminating the strained sections of the polymer chain.⁷⁴ At about 600–700°C, the residual weight fraction was caused by the experimental errors which was exactly concurrent with the Cu NPs loading in the PVP-fiber matrix (Figure 3a,b). Similar to the TGA curve analysis, the derivative of thermal degradation (DTG) indicates the correspondent dissociation of weight percentage loss with the temperature. At low temperature (up to 200°C), the rate of change of weight loss is constant indicating the zero-derivative portion in PEO fibers (Figure 3b), water just vaporized at a constant phase change. Thus, in this section, the polymer degradation is unnoticeable, probably reflecting negligible amounts of water still captured within the fibers. Reversely, for PVP fibers, more volatile ethanol gets easily dried within 120°C where the thermal degradation is quite fast (Figure 3d). Most importantly, the main degradation process occurs from about 225 to 450°C for PEO fibers while for PVP fibers, it is from 300 to 450°C. In this temperature range, the CuNPs are essentially shifting the degradation temperature slightly toward higher temperatures. It is observed in Figure 3b,d that the weight loss for all samples remains unchanged between 450 and 700°C, indicating that the decomposition of the polymer-fiber matrix is completed. The residual mass at 700°C is negligible for the pristine PEO and PVP fibers and consistent, within the experimental errors, with the content of CuNPs (near about 0 wt%) in the PEO and PVP fiber-matrices. The derivative of the residual mass as a function of temperature (Figure 3b,d) represents two negative degradation peaks in the various wt% of PEO and PVP fibers. These peaks are located at a temperature where the weight loss is maximum and eventually suggest two competing degradation mechanisms.⁷⁷ Basically, the incorporation of CuNPs in the PEO and PVP fibers narrows these peaks and shift them slightly to higher temperatures, signifying that CuNPs and polymer fibers are bonded adhesively, and dissociation temperature of both fibers are higher. At about 35 wt% of CuNPs, there are essentially a single major degradation peak at about 400°C and some minor broad peaks at lower temperatures.

3.4 | XRD results

Figure 4a shows the collected diffraction patterns for the PEO fibers, which are consistent with those reported by Takahasi and Tadokoro on PEO powder.⁷⁸ The Le bail fitting and determined lattice parameters are illustrated in Table 1. The fitting has a χ^2 of 1.70, which indicates a

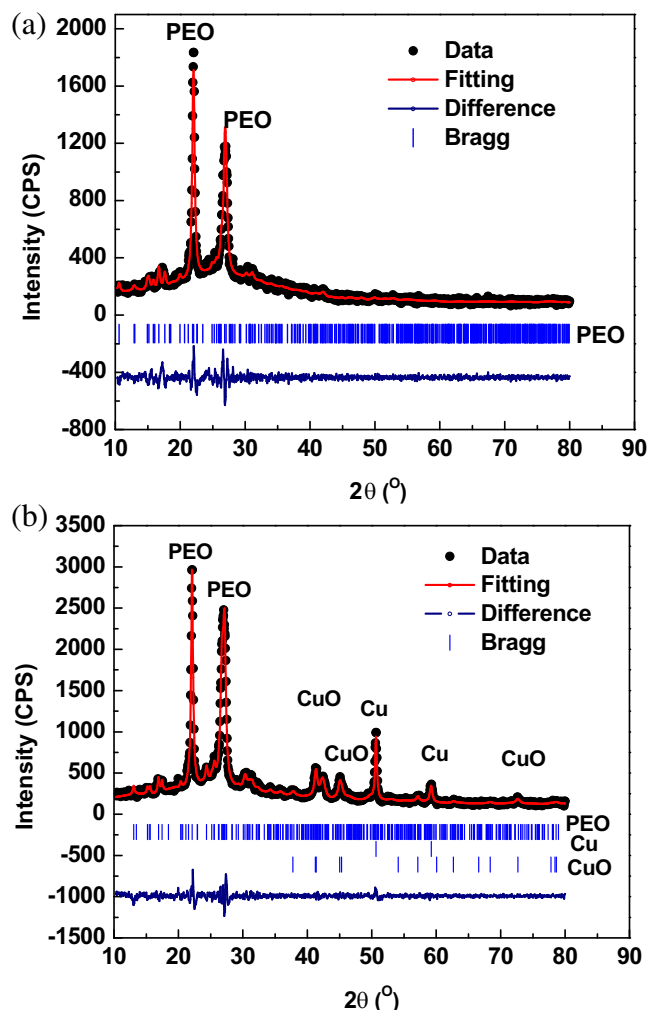


FIGURE 4 (a) Le bail fitting of the diffraction pattern collected for the PEO fibers. (b) Diffraction pattern collected for the PEO/Cu composite fibers. (c) Collected diffraction pattern of PVP fibers. (d) Le bail fitting of the PVP fibers with Cu NPs embedded in the fibers. Cu NPs, copper nanoparticles; PEO, polyethylene oxide; PVP, polyvinylpyrrolidone; SEM, scanning electron microscope [Color figure can be viewed at wileyonlinelibrary.com]

good agreement between the data of the crystal structure. The diffraction pattern for the PEO/Cu composite fibers (Figure 4b) confirms the presence of three phases (the two large diffraction PEO peaks at 22.08 and 26.94 in 2θ), Cu metal, and CuO. The CuO diffraction peaks observed in the sample represent the 110, 002/−111, 111/200, −202, and 113 planes, which were located at 37.710, 41.23, 41.38, 45.03, 45.31, and 73.64, in 2θ , respectively.⁷⁹ The Cu metal phase showed the 111 and 200 diffraction peaks, which were located at 50.28 and 59.213 in 2θ , respectively.⁸⁰ The Le bail fitting of the PEO-Cu composite fibers had a very good χ^2 value of 1.72 indicating a good agreement between the experimental data and fitting

The diffraction pattern of PVP fibers is shown in Figure 4c, which consisted of two diffuse-weak peaks located at 13.30 and 25.35 in 2θ . The XRD results of PVP fibers are consistent with those reported in the literature on PVP powder.⁸¹ The diffraction pattern was not fitted due to the amorphous phase present in the sample. The

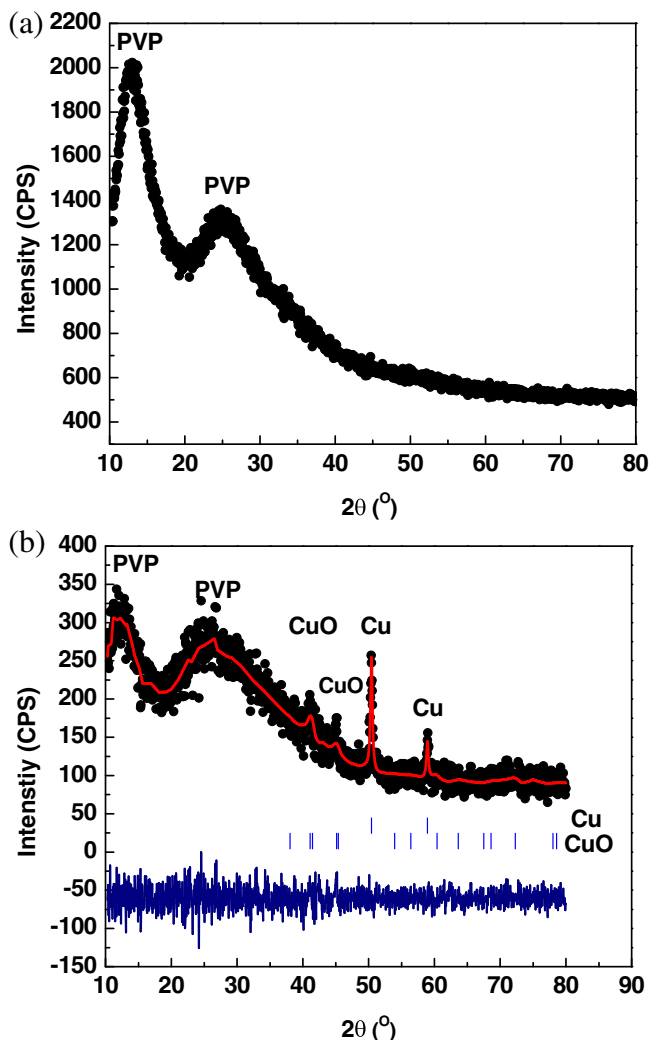


FIGURE 4 (Continued)

diffraction patterns of the PVP/Cu composite fibers are shown in Figure 4d. The diffraction pattern of the sample consisted of three phases: two PVP diffraction peaks at 13.30 and 25.35 in 2θ , CuO and Cu metal. The CuO phase showed the 002, -111 , 1211. The Cu 111 and 220 diffraction planes were observed in the Cu phase at 50.280 and 59.213 in 2θ , respectively. The Le Bail fitting results of the PVP/Cu composite fibers shown in Table 1 had a χ^2 of 1.35, again indicating an excellent agreement between the proposed phases and the experimental data.

3.5 | Antibacterial performance

As antibacterial agents, PEO/Cu and PVP/Cu nanofibrous membranes of different concentrations (15, 25, and 35 wt%) were tested for the antibacterial performance against the gram-negative *E. coli* and gram-positive *B. cereus* bacteria. In the disk diffusion method, fibers were kept on a cleaned agar plate contained with both bacteria for 72 h. Figure 5a–c shows the assessment of the growth of inhibition zone formation as an antimicrobial activity against *E. coli* by PEO/Cu (15, 25, and 35 wt%) while Figure 5d–f indicates activity by PVP/Cu (15, 25, and 35 wt%) composite nanofibrous membranes.

On the other hand, the growth of inhibition zone against *B. cereus* bacteria by PEO/Cu and PVP/Cu composite fibers are shown in Figure 5g–i,j–l, respectively.

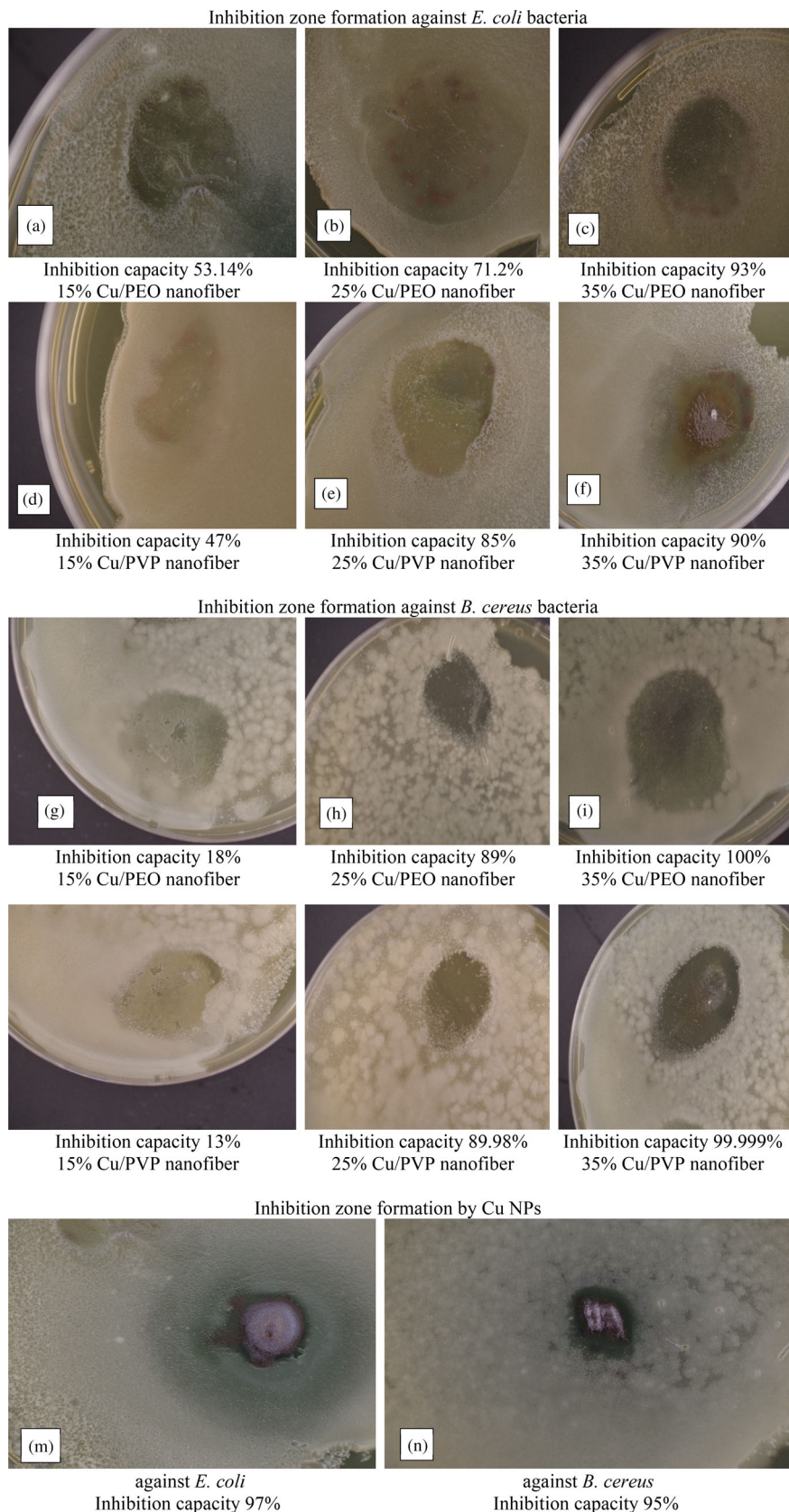
Finally, the antimicrobial activity of CuNPs was shown and its clear inhibition growth zones were indicated against in *E. coli* (Figure 5m) and *B. cereus* (Figure 5n). From the experimental data, it was observed that the inhibition zone growth against gram negative, *E. coli* bacteria in PEO/Cu composite fibers was 53.14%, 71.2%, and 93% for Cu concentration of 15, 25, and 35 wt%, respectively in 72 h (Figure 5a–c) where the average inhibition diameter was 1.64 out of 2.258 cm. Reversely, PVP/Cu fibers showed inhibition zone efficiency of 47, 85, and 90 for 15, 25, and 35 wt% Cu concentration presented in fibers, respectively. As a capping agent, Cu NPs can be

TABLE 1 Le bail fitting parameters for the PEO, PEO/CuNPs, and PVP/Cu NPs

Sample	Phase	Space group	a (Å)	b (Å)	c (Å)	α (°)	β (°)	γ (°)	χ^2
PEO	PEO	$P2_1/c$	8.00 (8)	13.20 (3)	19.53 (1)	90.00	123.89	90.00	1.70
PEO-Cu	PEO	$P2_1/c$	8.00 (8)	13.20 (3)	19.53 (1)	90.00	123.89	90.00	1.75
	CuO	$C2/c$	4.691 (5)	3.249 (2)	5.132 (3)	90.00	99.23	90.00	
	Cu	$FM\bar{3}M$	3.610 (1)	3.610 (1)	3.610 (1)	90.00	90.00	90.00	
PVP-Cu	CuO	$C2/c$	4.738 (6)	3.249 (3)	5.181 (4)	90.00	99.23	90.00	1.35
	Cu	$FM\bar{3}M$	3.638 (9)	3.638 (9)	3.638 (9)	90.00	90.00	90.00	

Abbreviations: Cu, copper; PEO, polyethylene oxide; PVP, polyvinylpyrrolidone.

FIGURE 5 Inhibition zone visible on the agar plate in PEO/Cu fibers of 15, 25, and 35 wt% nanoparticles. (a) Inhibition capacity 53.14% 15% Cu/PEO nanofiber. (b) Inhibition capacity 71.2% 25% Cu/PEO nanofiber. (c) Inhibition capacity 93% 35% Cu/PEO nanofiber. (d) Inhibition capacity 47% 15% Cu/PVP nanofiber. (e) Inhibition capacity 85% 25% Cu/PVP nanofiber. (f) Inhibition capacity 90% 35% Cu/PVP nanofiber. (g) Inhibition capacity 18% 15% Cu/PEO nanofiber. (h) Inhibition capacity 89% 25% Cu/PEO nanofiber. (i) Inhibition capacity 100% 35% Cu/PEO nanofiber. (j) Inhibition capacity 13% 15% Cu/PVP nanofiber. (k) Inhibition capacity 89.98% 25% Cu/PVP nanofiber. (l) Inhibition capacity 99.999% 35% Cu/PVP nanofiber. (m) against *E. coli* inhibition capacity 97%. (n) against *B. cereus* inhibition capacity 95%. Cu, copper; PEO, polyethylene oxide; PVP, polyvinylpyrrolidone [Color figure can be viewed at wileyonlinelibrary.com]



embedded effectively in PVP fibers at higher concentrations of Cu NPs. For this reason, the average inhibition diameter was 1.671 out of 2.258 cm in PVP/Cu nanofibrous membrane where bacteria grew less than PEO/Cu membrane. On the other hand, in gram-positive bacteria, *B. cereus* bacteria; the growth percentage of the inhibition zone capacity (Figure 5g–i) was 18%, 89%, and 100% in case of PEO/Cu fibers while for PVP/Cu fibers, Figure 5j–l, the inhibition zone capacity was 13%, 89.98%, and 99.99%. Moreover, the Cu NPs were proved as a good antibacterial agent since in CuNPs, *E. coli* and *B. cereus* bacteria were inhibited at 97% and 95% (Figure 5m,n) respectively.

From Figure 6, it is apparent that the inhibition capacity of PEO/Cu was higher than PVP/Cu nanofibrous membranes. Again, the inhibition zone formation on *E. coli* was more than for *B. cereus* as was observed in Figure 5 because the cell structural of gram *E. coli* is composed of thinner cell wall thickness of peptidoglycan while *B. cereus* is thicker cell wall, which is very hard to permeate.⁸² Within 72 h, *E. coli* was nearly fully inhibited by the membrane

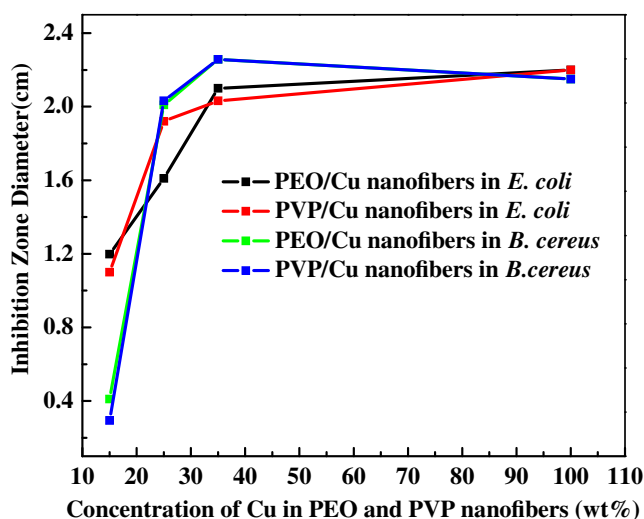


FIGURE 6 Relationship between Cu concentration in PEO/PVP nanofiber and corresponding inhibition zone diameter (the nanofiber's sample size was 2.258 cm). Cu, copper; PEO, polyethylene oxide; PVP, polyvinylpyrrolidone [Color figure can be viewed at wileyonlinelibrary.com]

while *B. cereus* was less inhibited than *E. coli*. Therefore, the PEO/Cu nanofibrous membranes were more effective to impede gram-negative bacterial strain where the strain can easily be paralyzed by fibers. However, the *B. cereus* bacterial strain was more capable to propagate alongside the nanofibrous membrane. Therefore, the inhibition zone efficiency in *B. cereus* was a bit lower than *E. coli*. (Table 2)

For the measurements of the inhibition zone diameter was taken after 3 days of inhibition of bacteria in the presence of composite fibers. The average inhibited zone diameter of PEO/Cu nanofibers on *E. coli* was then found to be 1.64 cm out of the sample diameter (2.258 cm) and in the case of *B. cereus* bacteria, the diameter was 1.6841 cm. Reversely, PVP/Cu fibrous membrane inhibition capacity (as an average diameter) was found to be 1.558 and 1.528 cm in *E. coli* and *B. cereus* bacteria, respectively. This antimicrobial function of nanofibrous membranes was due to the higher surface area to volume ratio of fibers dispersed into the homogeneous Cu NPs. Since Cu NPs have antibacterial activity with fibers, their function was visualized as indicated in Figure 5. Basically, Cu NPs were ionized as Cu^{2+} , which played a role to captivate the negative ion of cell structure and inactivate the DNA replication stability. As a result, both gram positive and negative bacteria were sterilized quickly. From the values illustrated in Table 1, it is evident that 35 wt% Cu NPs embedded in nanofibrous PEO and PVP membranes were a finer agent than other metallic oxides to inhibit bacteria.

3.6 | Cu NPs release and stability results

Cu NPs stability tests were performed to investigate the Cu^{2+} ion release from pure Cu NPs, Cu/PEO, and Cu/PVP composite fibers. Dissolution of Cu^{2+} ions from the different samples was investigated over 1 week with ultrapure water. The results for the Cu-NP sample (Figure 7a) showed that the Cu^{2+} concentration initially increased at 24 h, decreased after 48 h, and then increased continually up to 168 h. The observed decrease in the Cu^{2+} concentration might be due to the oxidation

TABLE 2 Inhibition zone diameter for the antibacterial activity of PEO/Ag fibers

Fibers in bacteria	Average diameter of inhibition zone (cm)	SD (mm)
PEO/Cu in <i>E. coli</i>	1.64 out of 2.258	0.45
PEO/Cu in <i>B. cereus</i>	1.6841 out of 2.258	0.51
PEO/Cu in <i>E. coli</i>	1.558 out of 2.258	1.005
PEO/Cu in <i>B. cereus</i>	1.528 out of 2.258	1.0749

Abbreviations: Cu, copper; PEO, polyethylene oxide.

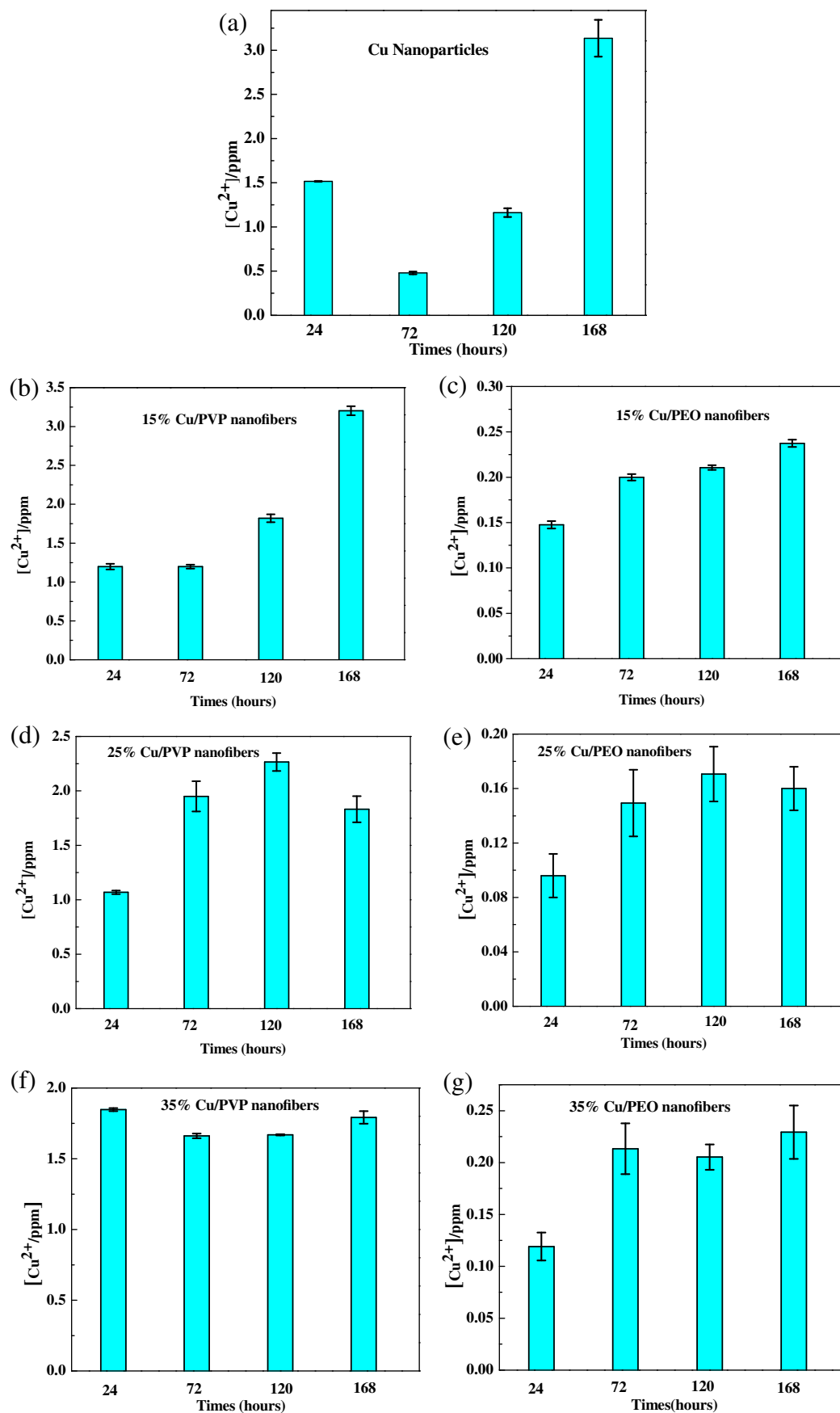


FIGURE 7 Legend on next page.

of the Cu-NP surface, which would generate binding sites on the NPs. These binding sites may then have led to an adsorption of free Cu^{2+} ions from the solution onto the NP surface. The dissolution processes should overcome the surface complexation over time, hence resulting in an increased release of Cu^{2+} . It can be observed in Figure 7 B that the 15 wt% PVP/Cu composite-fiber-sample showed an increase in Cu^{2+} concentration with increasing time, which reached a maximum value at 168 h. However, the 15 wt% PEO/Cu composite fibers showed a similar trend of increasing Cu^{2+} concentration with increasing time (Figure 7c). As can be seen in Figure 7d, e, both the 25 wt% PVP/Cu and PEO/Cu composite-fiber samples showed a similar behavior of increasing concentration with increasing time. However, the 25 wt% samples reached maximum of Cu^{2+} concentration in solution faster than the 15 wt% samples, with 72 h of reaction. The 35 wt% PVP/Cu composite-fiber sample showed a different behavior compared to other samples. Within the first 24 h of the study, the maximum concentration of Cu^{2+} was released while the concentration remained constant up to the 168 h, as can be seen in Figure 7f. The 35 wt% PEO/Cu samples showed a similar behavior to that of the 25 wt% PEO/Cu composite fibers where an increasing in Cu^{2+} concentration was observed at increasing time while equilibrium was reached within the first 72 h and remained constant thereafter. It should also be noted that the PEO/Cu composite-fiber samples consistently had a lower dissolution of Cu NPs as can be seen by the low concentration of Cu^{2+} in solution, which maximized at 0.25 ppm. On the other hand, the Cu-NP sample reached a maximum consideration of Cu^{2+} at approximately 3 ppm while the 15%, 25%, and 35% PVP/Cu composite-fiber samples showed a maximum of Cu^{2+} concentration at approximately 3.0, 2.25, and 1.8 ppm, respectively. The difference in behavior between the PVP/Cu, PEO/Cu, and Cu-NPs samples can be explained by the attachment of surface groups to the Cu NPs. The Cu-NP samples do not have a surfactant covering the NPs, which makes them readily available for dissolution. However, the PVP and PEO in the PVP/Cu and PEO/Cu composite fibers act as surfactants on the NP surface and aid in slowing or reducing the dissolution of Cu^{2+} ions. In fact, PVP has a terminal ketone group in its backbone, which does not bind to metal ions or particles very easily. On the other hand, PEO has terminal alcohol groups, which can bind to the copper through removing

the hydrogen group. The formation constants for Cu to PVP are approximately 10 in a tetra coordinate system while it is approximately 16 for Cu to PEO.^{83,84} As can be seen in the stability data, the PEO/Cu type complex is much stronger than that for the PVP/Cu and could account for the lower solubility observed in the current study.

4 | CONCLUSION

PEO/Cu and PVP/Cu composite fibers were fabricated by centrifugal spinning of PEO/Cu/water and PVP/Cu/ethanol precursor solutions, respectively. In this processing method, the spinneret speed (5500 rpm for PEO/Cu and 7000 rpm for PVP/Cu), favorable relative humidity (46%) and concentrations for both solutions (8 wt% for PEO/Cu and 18 wt% for PVP/Cu) were the interplay to obtain fine morphological fibrous mats. The structure and morphological characterization of the fibers were performed by SEM EDS, XRD, which indicated the presence of distributed Cu NPs throughout the nanofibrous membranes where 15, 25, and 35 wt% Cu NPs were vividly embedded in both composite fibers. For the antibacterial tests, a disk diffusion method was performed while inhibition zone for six samples (three for each composite fibers) was detected accurately. During the Cu release study, Cu NPs dissociate to Cu^{2+} ion properly; assisting the microbial function of the nanofibrous membrane to be implemented in bacterial cell effectively. For this reason, in agar plate medium, in case of gram-negative *E. coli*; the inhibition zone efficiency was near about 91.5% for the both composite fibers at 35 wt% concentration of Cu NPs in the fiber-matrix. On the other hand, for gram-positive bacteria *B. cereus*, 35 wt% Cu concentration in both nanofiber samples showed 100% inhibition efficiency. This was possible due to the high-surface area to volume ratio based on which befitting Cu NPs were dispersed into fibrous mats. Basically, centrifugally spun fibers were very porous in nature where Cu NPs can be capped very easily. In effect, more Cu NPs were distributed on the surface of membranes and played a role to inactivate the bacterial cell membrane efficiently. Hopefully in future, both PEO/Cu and PVP/Cu nano-fibrous membranes could be a noticeable treatment from the exemption of the bacterial strains.

FIGURE 7 Concentration of Cu^{2+} released from Cu NPs sample as a function of the immersion time. (a) Figure is for Cu^{2+} release. (b and c) Indicating 15% Cu^{2+} released from PVP/Cu and PEO/Cu fibers respectively. (d and e) Indicates 25% Cu^{2+} released from PVP/Cu and PEO/Cu fibers respectively. (f and g) Indicates 35% Cu^{2+} released from PVP/Cu and PEO/Cu fibers respectively. Cu, copper; PEO, polyethylene oxide; PVP, polyvinylpyrrolidone [Color figure can be viewed at wileyonlinelibrary.com]

To the best of the authors' knowledge, this is the first results to be reported on the centrifugal spinning of Cu/PEO and Cu/PVP composite fibers for use as antibacterial agents against bacteria.

ACKNOWLEDGMENT

This work was also supported by National Science Foundation (NSF) PREM award under grant no. DMR-2122178: UTRGV-UMN Partnership for Fostering Innovation by Bridging Excellence in Research and Student Success. Acknowledge the Bensen Endowment in Engineering. Partial support was provided by the Lloyd M. Bentsen, Jr. Endowed Chair in Engineering endowment at UTRGV.

ORCID

Mataz Alcoutlabi  <https://orcid.org/0000-0003-4641-9109>

REFERENCES

- Z. Zhang, Y. Wu, Z. Wang, X. Zou, Y. Zhao, L. Sun, *Mater. Sci. Eng., C* **2016**, *69*, 462.
- M. Derrien, J. E. van Hylckama Vlieg, *Trends Microbiol.* **2015**, *23*, 354.
- J. Quirós, J. P. Borges, K. Boltes, I. Rodea-Palomares, R. Rosal, *J. Hazard. Mater.* **2015**, *299*, 298.
- G. Broughton II., J. E. Janis, C. E. Attinger, *Plast. Reconstr. Surg.* **2006**, *117*, 6S.
- K. M. Sawicka, P. Gouma, *J. Nanopart. Res.* **2006**, *8*, 769.
- N. P. Desai, J. A. Hubbell, *ACS* **1990**, *62*, 731.
- Q. P. Pham, U. Sharma, A. G. Mikos, *Tissue Eng.* **2006**, *12*, 1197.
- N. Khanam, C. Mikoryak, R. K. Draper, K. J. Balkus Jr., *Acta Biomater.* **2007**, *3*, 1050.
- S. Kumbar, R. James, S. Nukavarapu, C. Laurencin, *Biomed. Mater.* **2008**, *3*, 034002.
- B.-M. Min, G. Lee, S. H. Kim, Y. S. Nam, T. S. Lee, W. H. Park, *Biomaterials* **2004**, *25*, 1289.
- M. Mattioli-Belmonte, A. Zizzi, G. Lucarini, F. Giantomassi, G. Biagini, G. Tucci, F. Orlando, M. Provinciali, F. Carezzi, P. Morganti, *J. Bioact. Compat. Polym.* **2007**, *22*, 525.
- D. G. Castner, B. D. Ratner, *Surf. Sci.* **2002**, *500*, 28.
- R. Rani, H. Kumar, R. Salar, S. Purewal, *Int. J. Pharm. Res. Dev.* **2014**, *6*, 72.
- Š. Zupančič, L. Preem, J. Kristl, M. Putrinš, T. Tenson, P. Kocbek, K. Kogermann, *Eur. J. Pharm. Sci.* **2018**, *122*, 347.
- J. Pelipenko, P. Kocbek, J. Kristl, *Eur. J. Pharm. Sci.* **2015**, *66*, 29.
- H. Matsumoto, A. Tanioka, *Membranes* **2011**, *1*, 249.
- K. Balasubramanian, K. M. Kodam, *RSC Adv.* **2014**, *4*, 54892.
- K. Balasubramanian, R. Yadav, P. Prajith, *Int. J. Plast. Technol.* **2015**, *19*, 363.
- D. Pamfil, E. Butnaru, C. Vasile, *J. Polym. Res.* **2016**, *23*, 146.
- R. S. Ambekar, B. Kandasubramanian, *Biomater. Sci.* **2019**, *7*, 1776.
- H. Liu, Y. Zhou, S. Chen, M. Bu, J. Xin, S. Li, *Asian J. Pharm. Sci.* **2013**, *8*, 269.
- Q. Liu, J. Huang, H. Shao, L. Song, Y. Zhang, *RSC Adv.* **2016**, *6*, 7683.
- C. Huang, Y. Ouyang, H. Niu, N. He, Q. Ke, X. Jin, D. Li, J. Fang, W. Liu, C. Fan, *ACS Appl. Mater. Interfaces* **2015**, *7*, 7189.
- M. Abrigo, S. L. McArthur, P. Kingshott, *Macromol. Biosci.* **2014**, *14*, 772.
- F. E. Ahmed, B. S. Lalia, R. J. D. Hashaikeh, *Desalination.* **2015**, *356*, 15.
- X. Li, W. Chen, Q. Qian, H. Huang, Y. Chen, Z. Wang, Q. Chen, J. Yang, J. Li, Y. W. J. A. E. M. Mai, *Adv. Energy Mater.* **2021**, *11*, 2170010.
- V. A. Agubra, L. Zuniga, D. De la Garza, L. Gallegos, M. Pokhrel, M. Alcoutlabi, *Solid State Ionics* **2016**, *286*, 72.
- L. Zuniga, G. Gonzalez, R. O. Chavez, J. C. Myers, T. P. Lodge, M. Alcoutlabi, *Appl. Sci.-Basel* **2019**, *9*, 4032.
- L. Zuniga, V. Agubra, D. Flores, H. Campos, J. Villareal, M. Alcoutlabi, *J. Alloy Compd.* **2016**, *686*, 733.
- N. Obregon, V. Agubra, M. Pokhrel, H. Campos, D. Flores, D. De la Garza, Y. B. Mao, J. Macossay, M. Alcoutlabi, *Fibers* **2016**, *4*, 1. <https://doi.org/10.3390/fib4020020>.
- R. O. Chavez, T. P. Lodge, J. Huitron, M. Chipara, M. Alcoutlabi, *J. Appl. Polym. Sci.* **2021**, *138*, e50396.
- D. De la Garza, F. De Santiago, L. Materon, M. Chipara, M. Alcoutlabi, *J. Appl. Polym. Sci.* **2019**, *136*, e47480.
- S. S. H. Abir, M. T. Hasan, M. Alcoutlabi, K. Lozano, *Fiber Polym.* **2021**, *22*. <https://doi.org/10.1007/s12221-021-1059-x>
- J. Lopez, R. Gonzalez, J. Ayala, J. Cantu, A. Castillo, J. Parsons, J. Myers, T. P. Lodge, M. Alcoutlabi, *J. Phys. Chem. Solids* **2021**, *149*. <https://doi.org/10.1016/j.jpcs.2020.109795>.
- A. S. Nain, M. Sitti, A. Jacobson, T. Kowalewski, C. Amon, *Macromol. Rapid Commun.* **2009**, *30*, 1406.
- J. Zhao, W. Han, H. Chen, M. Tu, R. Zeng, Y. Shi, Z. Cha, C. Zhou, *Carbohydr. Polym.* **2011**, *83*, 1541.
- D. Paneva, F. Bougard, N. Manolova, P. Dubois, I. Rashkov, *Eur. Polym. J.* **2008**, *44*, 566.
- D. Li, Y. N. Xia, *Adv. Mater.* **2004**, *16*, 1151.
- C. Saiyasombat, S. Maensiri, *J. Polym. Eng.* **2008**, *28*, 5.
- T. Hou, X. Li, Y. Lu, B. Yang, *Mater. Des.* **2017**, *114*, 303.
- R. O. Chavez, T. P. Lodge, M. Alcoutlabi, *Mater. Sci. Eng. B-Adv.* **2021**, *266*. <https://doi.org/10.1016/j.mseb.2020.115024>.
- M. T. Hasan, R. Gonzalez, M. Chipara, L. Materon, J. Parsons, M. Alcoutlabi, *Polym. Adv. Technol.* **2021**, *32*, 2327.
- J. L. Lumley, *Ann. Rev. Fluid Mech.* **1969**, *1*, 367.
- S. Siggia, *J. Am. Pharm. Assoc. (Sci. Ed.)* **1957**, *46*, 201.
- I. Iliopoulos, J. Halary, R. Audebert, *J. Polym. Sci., Part A: Polym. Chem.* **1988**, *26*, 275.
- C.-I. Ren, R. Nap, I. Szeleifer, *J. Phys. Chem. B* **2008**, *112*, 16238.
- N. P. Desai, J. A. Hubbell, *J. Biomed. Mater. Res.* **1991**, *25*, 829.
- K.-H. Cho, J.-E. Park, T. Osaka, S.-G. Park, *Electrochim. Acta* **2005**, *51*, 956.
- H. Savaş, O. Güven, *Int. J. Pharm.* **2001**, *224*, 151.
- I. Kohsari, Z. Shariatinia, S. M. Pourmortazavi, *Carbohydr. Polym.* **2016**, *140*, 287.
- K. H. Jung, M. W. Huh, W. Meng, J. Yuan, S. H. Hyun, J. S. Bae, S. M. Hudson, I. K. Kang, *J. Appl. Polym. Sci.* **2007**, *105*, 2816.
- S. Selvam, M. Sundrarajan, *Carbohydr. Polym.* **2012**, *87*, 1419.

- [53] F. Yalcinkaya, M. Komarek, D. Lubasova, F. Sanetnik, J. Maryska, *J. Nanomater.* **2016**, 2016. <https://doi.org/10.1155/2016/7565972>.
- [54] M. Karpuraranjith, S. Thambidurai, *Int. J. Biol. Macromol.* **2017**, 104, 1753.
- [55] R. Bryaskova, D. Pencheva, S. Nikolov, T. Kantardjiev, *J. Chem. Biol.* **2011**, 4, 185.
- [56] F. Yalcinkaya, D. Lubasova, *Polym. Adv. Technol.* **2017**, 28, 137.
- [57] G. Ren, D. Hu, E. W. Cheng, M. A. Vargas-Reus, P. Reip, R. P. Allaker, *Int. J. Antimicrob. Agents* **2009**, 33, 587.
- [58] J. P. Ruparelia, A. K. Chatterjee, S. P. Dutttagupta, S. Mukherji, *Acta Biomater.* **2008**, 4, 707.
- [59] M. Gondwal, G. J. N. Pant, *Int. J. Biomater.* **2018**, 2018, 6735426.
- [60] S. M. Briffa, I. Lynch, V. Trouillet, M. Bruns, D. Hapiuk, J. Liu, R. Palmer, E. Valsami-Jones, *RSC Adv.* **2017**, 7, 3894.
- [61] M. Shahmiri, N. A. Ibrahim, F. Shayesteh, N. Asim, N. Motallebi, *J. Mater. Res.* **2013**, 28, 3109.
- [62] D. Flores, J. Villarreal, J. Lopez, M. Alcoutlabi, *Mater. Sci. Eng. B-Adv.* **2018**, 236, 70.
- [63] M. R. Badrossamay, H. A. McIlwee, J. A. Goss, K. K. Parker, *Nano Lett.* **2010**, 10, 2257.
- [64] S. Thenmozhi, N. Dharmaraj, K. Kadirvelu, H. Y. Kim, *Mater. Sci. Eng., B* **2017**, 217, 36.
- [65] S. Padron, R. Patlan, J. Gutierrez, N. Santos, T. Eubanks, K. Lozano, *J. Appl. Polym. Sci.* **2012**, 125, 3610.
- [66] B. C. Weng, F. H. Xu, G. Garza, M. Alcoutlabi, A. Salinas, K. Lozano, *Polym. Eng. Sci.* **2015**, 55, 81.
- [67] A. Hoffmann, A. J. C. Kuehne, *Polymers* **2021**, 13. <https://doi.org/10.3390/polym13081313>.
- [68] S. Mei, X. Feng, Z. Jin, *Soft Matter* **2013**, 9, 945.
- [69] R. Weitz, L. Harnau, S. Rauschenbach, M. Burghard, K. Kern, *Nano Lett.* **2008**, 8, 1187.
- [70] Z.-M. Zhang, Y.-S. Duan, Q. Xu, B. Zhang, *J. Eng. Fibers Fabr.* **2019**, 14, 1558925019867517.
- [71] Z. Li, S. Mei, Y. Dong, F. She, L. Kong, *Polymer* **2019**, 11, 1550.
- [72] C. Liu, J. Sun, M. Shao, B. Yang, *RSC Adv.* **2015**, 5, 98553.
- [73] K. Shameli, M. B. Ahmad, A. Zamanian, P. Sangpour, P. Shabanzadeh, Y. Abdollahi, M. Zargar, *Int. J. Nanomed.* **2012**, 7, 5603.
- [74] V. Bogatyrov, N. Borisenko, V. Pokrovskii, *Russ. J. Appl. Chem.-Eng. Tr* **2001**, 74, 839.
- [75] H. M. Ng, N. M. Saidi, F. S. Omar, R. Kasi, R. T. Subramaniam, S. Baig, *Therm. Anal. Polym.*, **2018**, 1. <https://doi.org/10.1002/0471440264.pst667>
- [76] M. Polaskova, P. Peer, R. Cermak, P. Ponizil, *Polymer* **2019**, 11, 1384.
- [77] J. Hou, Y. Wang, H. Xue, Y. Dou, *Polymer* **2018**, 10, 1032.
- [78] Y. Takahashi, H. Tadokoro, *Macromolecules* **1973**, 6, 672.
- [79] S. Åsbrink, L.-J. Norrby, *Acta Crystallogr., Sect. B: Struct. Crystallogr. Cryst. Chem.* **1970**, 26, 8.
- [80] I.-K. Suh, H. Ohta, Y. Waseda, *J. Mater. Sci.* **1988**, 23, 757.
- [81] X.-f. Qian, J. Yin, S. Feng, S.-h. Liu, Z.-k. Zhu, *J. Mater. Chem.* **2001**, 11, 2504.
- [82] S. Sriskandan, J. Cohen, *Infect. Dis. Clin. North Am.* **1999**, 13, 397.
- [83] H. Nishikawa & E. J. T. J. O. P. C. Tsuchida Complexation and form of poly (vinylpyridine) derivatives with copper (II) in aqueous solution. 1975, 79, 2072.
- [84] W. M. Hosny, P. A. J. I. J. E. S. Khalaf-Alaa, Potentiometric study and biological activity of some metal ion complexes of polyvinyl alcohol (PVA). **2013**, 8, 1520.

How to cite this article: M. T. Hasan, R. Gonzalez, A. A. Munoz, L. Materon, J. G. Parsons, M. Alcoutlabi, *J. Appl. Polym. Sci.* **2021**, e51773. <https://doi.org/10.1002/app.51773>